Cancer Letters 445 (2019) 11–23

Contents lists available at ScienceDirect

Cancer Letters

journal homepage: www.elsevier.com/locate/canlet

Original Articles

Novel selective TOPK inhibitor SKLB-C05 inhibits colorectal carcinoma growth and metastasis

Tiantao Gao[a,1], Quanfang Hu[a,1], Xi Hu[a], Qian Lei[a], Zhanzhan Feng[a], Xi Yu[c], Cuiting Peng[b], Xuejiao Song[d], Hualong He[b], Ying Xu[a], Weiqiong Zuo[a], Jun Zeng[a], Zhihao Liu[a,**], Luoting Yu[a,*]

[a] State Key Laboratory of Biotherapy and Cancer Center, West China Hospital, West China Medical School, Sichuan University, Collaborative Innovation Center for Biotherapy, 17 #3rd Section, Ren Min South Road, Chengdu, 610041, China
[b] School of Chemical Engineering, Sichuan University, Chengdu, 610041, China
[c] Carey Business School, Johns Hopkins University, Baltimore, MD, 21202, USA
[d] Research Center for Public Health and Preventive Medicine, West China School of Public Health, Sichuan University, Chengdu, Sichuan, China

ARTICLE INFO

Keywords:
MAPK signaling pathway
Mitosis failure
DNA-reparation failure
FAK signaling
Apoptosis

ABSTRACT

The mitogen-activated protein kinase (MAPK) signaling pathway member T-LAK cell–originated protein kinase/PDZ-binding kinase (TOPK/PBK) is closely involved in tumorigenesis and progression. Its overexpression in colorectal carcinoma (CRC) exacerbates tumor malignancy, promotes metastasis and results in dismal prognosis. Therefore, targeting TOPK is a promising approach for CRC therapy. Here, we report the development of a TOPK selective inhibitor SKLB-C05, with subnanomolar inhibitory potency. In vitro, SKLB-C05 exhibited excellent cytotoxicity and anti-migration and invasion activity on TOPK high-expressing CRC cells and induced cell apoptosis. These activities could attribute to its inhibition of TOPK downstream signaling including extracellular signal-regulated kinase 1/2 (ERK1/2), p38, and c-Jun N-terminal kinase 1, 2, and 3 (JNK1/2/3), as well as downregulation of FAK/Src- MMP signaling. Furthermore, SKLB-C05 disrupted cell mitosis and blocked CRC cell cycle. In vivo, oral administration of SKLB-C05 at concentrations of 20 and 10 mg kg^{-1}·day^{-1} dramatically attenuated CRC tumor xenograft growth and completely suppressed hepatic metastasis of HCT116 cells, respectively. Thus, these findings suggest that SKLB-C05 is a specific TOPK inhibitor with potent anti-CRC oncogenic activity *in vitro* and *in vivo*.

1. Introduction

PBK/TOPK, a serine-threonine kinase, is a member of the MAPK kinase (MAPKK) family [1], and the MAPKK signaling pathway is a component of the RAS/RAF/MAPKK [MEK]/ERK signaling axis. The evolutionary branch of TOPK is between that of MEK1/2 and MKK7 while it is closer to MEK1/2 [2], and TOPK is known as a downstream target of EWS-FLI1 chimeric fusion protein [3]. PBK/TOPK was initially identified as a mitotic-related protein kinase that phosphorylated histone H3 at Ser10, which are important for cytokinesis and cell proliferation [4–6]. Furthermore, during mitosis, TOPK and the cyclin B1/CDK1 complex promote cytokinesis through the phosphorylation of PRC1 [7,8]. Previous report indicated that positive feedback between TOPK and ERK2 promotes colorectal cancer (carcinoma, CRC) formation. TOPK was reported to activate the p38 pathway to help cancer cells surmount DNA damage [9] and TOPK was reported to correspond with ultraviolet B (UVB)-induced JNK activation [10]. Furthermore, it can also promote tumorigenesis by inhibiting p53 and its downstream target [11]. In this context, TOPK serves as an upstream activator of MAPK and mitosis relevant kinase, and plays a pivotal role in cancer-advancing activities such as tumor proliferation, apoptosis, inflammation, and metastasis [10,12–15]. TOPK was reported aberrantly expressed in cancers such as CRC [16], breast [17], prostate [18], lung [19], and cholangiocarcinoma [20], etc.

CRC is one of the most common cancer types worldwide. According to the statistics of the American Cancer Society in 2018, it was estimated that CRC cases accounted for 8% of 1,735,350 increased patients with cancer, and the rate of CRC-related deaths accounted for 8% of the

* Corresponding author. Lab of Medicinal Chemistry, State Key Laboratory of Biotherapy and Cancer Center, West China Hospital, Sichuan University and Collaborative Innovation Center for Biotherapy, 17#3rd Section, Ren Min South Road, Chengdu, 610041, China.
** Corresponding author.
E-mail addresses: liuzhihao@scu.edu.cn (Z. Liu), yuluot@scu.edu.cn (L. Yu).
[1] These authors contribute equally to this work.

https://doi.org/10.1016/j.canlet.2018.12.016
Received 8 August 2018; Received in revised form 8 December 2018; Accepted 11 December 2018

estimated cancer-related moralities [21]. There is a need and an opportunity to identify new targets for both the prevention of CRC and development of effective therapies [22]. After estimating the prognostic value of TOPK in 2000 cases of CRC, ZlobecI et al. [23] proposed that cases with high expression of TOPK are associated with poor prognosis and tolerance to tyrosine kinase inhibitors, and TOPK inhibition would benefit 30–40% of patients with CRC.

Additionally, as a major factor responsible for poor prognosis, metastasis of CRC demonstrates tissue and organ specificity [24]. The liver, lung, and lymph nodes are the main metastasis sites, and liver metastasis is the most common and major cause of death in patients with CRC [25]. TOPK was reported to be closely correlated with metastasis in numerous types of cancers [18,26], therefore, its suppression is expected to attenuate metastasis of CRC. Studies have indicated that TOPK induced metastasis via β-catenin-mediated MMP production [27], or modulation of signaling such as the PI3K/PTEN/AKT pathway [19]. However, we found that FAK, which plays important roles in cell adhesion and migration [28], also functions in TOPK-mediated metastasis.

TOPK has been confirmed to have an oncogenic role in CRC, especially in patients with tolerance to other tyrosine kinase inhibitors [29], therefore, the development of specific inhibitors would be appropriate for CRC treatment. Although several extracts and novel small-molecule inhibitors have been found to act by inhibiting the activity of TOPK [30–36], there is still necessity to develop more selective and effective TOPK inhibitors. Our previous screening experiment discovered the compound (R)-1-(4-(1-aminopropan-2-yl) phenyl)-2-hydroxy-4-methylphenanthridin-6(5H)-one hydrochloride (SKLB-C05) as a potent TOPK inhibitor. SKLB-C05 demonstrated excellent *in vitro* inhibitory activity against TOPK kinase and *in vitro* cellular assays revealed that it selectively and strongly inhibited TOPK-positive CRC cell proliferation and migration through the inhibition of TOPK-regulated signaling pathways. Moreover, we found that SKLB-C05 suppressed tumor growth in CRC xenograft mouse model and inhibited the hepatic metastasis in HCT116 model. Taken together, our data indicated that SKLB-C05 could be a superior TOPK inhibitor for the treatment of CRC and provide a foundation for further investigation.

2. Materials and methods

2.1. Solubility and log D test

In order to determine the solubility of this compound, a sufficient amount of compound was added to the solvent. After 30 min of sonication, the solution was shaken at 37 °C water bath for 24 h to form a supersaturated solution. Then the solution was filtrated and diluted, and the final concentration, which is solubility of compound, was determined by HPLC.

LogD value is used to evaluate the lipophilicity of a compound, which is an important determinant of most drug properties. $1 < \text{Log } D_{7.4} < 3$ is an ideal range. These compounds generally have good intestinal absorption, owing to a good balance of solubility and passive diffusion permeability. To test the Log $D_{7.4}$ of SKLB-C05, the compound was added to a mixed solution of n-octanol and 10 mM phosphate buffer (pH 7.4), and the mixture was stirred overnight at room temperature. The aqueous phase and the organic phase were separated, filtered and diluted for appropriate times, and the compound concentration in organic phase and the aqueous phase were determined by HPLC respectively. The distribution ratio was calculated to get Log D value, and Log D value is calculated according to the following formula:

$$\text{Log } D_{pHx} = \log([\text{Compound}_{organic}] \,/\, [\text{Compound}_{aqueous}])$$

Log D of the compound between an organic phase (e.g., octanol) and an aqueous phase (e.g., buffer) at a specified pH (x).

2.2. Kinase assay

Inhibition of kinase activity by the compounds SKLB-C05 was assessed against TOPK and a panel of other 368 diverse human protein kinases by Reaction Biology Corp. Activity of individual protein kinases was assessed by the Hot Spot assay platform, which contains specific kinase/substrate pairs along with required cofactors [37]. The reaction mixture containing the compound and ^{33}P-ATP was incubated at room temperature for 2 h and spotted onto P81 ion exchange paper. The kinase activity was measured as ^{33}P intensity of the spots. The extent of the kinase activity was expressed as a percentage relative to the kinase activity obtained in the absence of the compound. The percent inhibition by the compound was then defined as the percentage by which kinase activity decreases in the presence of the compound.

2.3. Thermal shift assay

Thermal shift assay was concluded to evaluate whether SKLB-C05 binds with TOPK protein. HCT116 cells were harvested, washed with PBS, and then lysed by RIPA lysis buffer containing cocktail (1:1000) and scraped by cell scraper to move into the tube. The soluble fraction (lysate) was separated from the cell debris by centrifugation at13000 rpm at 4 °C for 20 min. The cell lysates were divided into two aliquots, with one aliquot being treated with SKLB-C05 (10 μM) and the other aliquot with control. After 30 min of incubation at room temperature, the respective lysates were divided into smaller (50 μL) aliquots and heated individually at different temperatures (45, 50, 55, 60, 65, 70, 85, 100 °C) for 6 min to determine the degradation temperature of TOPK protein under SKLB-C05 or control treatment, followed by cooling at room temperature for 3 min. Then the heated lysates were centrifuged at 20000 rpm at 4 °C for 20 min in order to remove the denatured proteins. 20 μL of supernatants were transferred to new microtubes and analyzed by immunoblotting analysis [38].

2.4. Cell culture and regents

All cell lines were purchased from American Type Culture Collection (ATCC). Human colon cancer cell Colo205 were cultured in minimum Eagle's medium (MEM) media supplemented with 20% fetal bovine serum (FBS) and Penicillin-Streptomycin under humidified conditions with 5% CO_2 at 37 °C, and other CRC cells were cultured in Rosewell Park Memorial Institute (RPMI) 1640 media supplemented with 10% FBS and Penicillin-Streptomycin under humidified conditions with 5% CO_2 at 37 °C.

2.5. Cell proliferation and colony formation assay

Cells were seeded ($\sim 1 \times 10^3$ cells per well) in 96-well plates and incubated for 24 h and then treated with different doses of the compound. After indicated times, cell viability was determined using an MTT (Sigma-Aldrich, St. Louis, MO, USA) assay. The IC_{50} values were calculated using the GraphPad Prism 7 software. For the colony formation assay, cells were treated with SKLB-C05 for 14 days, fixed with 4% paraformaldehyde, and then stained with 0.05% crystal violet. Then, the images were captured under an inverted microscope, and colonies > 50 cells (analyzed by Image J) were counted.

2.6. Wound healing and cell invasion assay

HCT116 and SW480 cells were allowed to grow into full confluence in 12-well plates and then scratched by pipette tips and washed with PBS. Then complete medium with different concentrations of SKLB-C05 or vehicle were added in. Images were taken by an OLYMPUS inverted digital camera after 24 h incubation. Transwell assay was conducted as the protocol. Briefly, the upper chambers of 24-well transwell plates (Millipore) were coated with matrigel diluted in serum-free medium

(1:4) while the lower chambers were filled with 600 μL of complete medium. After the matrigel polymerization, the cells in serum-free medium added with indicated doses of SKLB-C05 were placed in the upper chambers. After a 24 h's incubation, the non-migrated cells were removed from the upper side of the filter, and the migrated cells were fixed with 4% paraformaldehyde and stained with 0.05% crystal violet. Images were taken using a ZEISS digital microscope and invading cells were counted by manual counting.

2.7. Cell cycle and apoptosis analysis

The cell cycle and apoptosis assays were both conducted on flow cytometry (FCM), and before analysis, cells were treated by SKLB-C05 for 48 h. For cell cycle analysis, cells were harvested and washed thrice, fixed by 70% ethanol and then stained with PI staining solution for 10 min in dark for analysis. For apoptosis analysis, cells were harvested and stained by an Annexin V− Fluorescein isothiocyanate (FITC) apoptosis detection kit (Roche, Indianapolis, IN, USA) according to the manufacturer's protocol. The data were analyzed by NovoExpress 1.1.2 Software.

2.8. Immunoblotting analysis

Cells were treated by SKLB-C05 for indicated time. Then harvested cells were lysed in RIPA buffer (Beyotime, Beijing, China) contained cocktail (1:1000) and phosphatase inhibitors (Roche, Basel, CH) for 30 min and equalized before loading. The samples were separated on SDS-PAGE gel and transferred onto nitrocellulose (NC) filter membranes (Merck Millipore, MS, USA). Then the membranes were incubated with appropriate primary antibody and corresponding secondary antibody. Specific protein bands were detected via chemiluminescence detection. The antibodies used in this article are listed in the Supplementary Tab. S1.

2.9. Quantitative real time-PCR (qRT-PCR) analysis

The CRC cells were treated with different dose of SKLB-C05 and control. Total cellular RNAs were extracted 48 h after treated by SKLB-C05. RNAs were reverse transcribed into cDNA with the Gene touch System (Bioer, CN) according to the manufacturer's protocol (Mei 5 Biotechnology, Co., Ltd). Q RT-PCR analysis of p21 and p53 gene expression was carried out using SYBR Green RT-PCR Kit from Takara on a BIO-RAD CFX96 Real-Time PCR System, according to the manufacturer's instructions. The PCR primer sequences for p21: forward 5' – GGCAGACCAGCATGACAGATT-3′ and reverse 5′ GCGGATTAGGGCTT CCTCTT - 3'; primer for p53: forward 5′-ACCAGGGCAGCTACGGTTTC - 3′ and reverse 5' -CCTGGGCATCCTTGAGTTCC- 3'; primer for GAPDH: forward 5' – GAAGGTGAAGGTCGGAGTC-3′ and reverse 5' – GAAGAT GGTGATGGGATTTC-3'.

2.10. Immunofluorescence (IF) and immunohistochemistry (IHC) analysis

The IF and IHC analyses were conducted according to standard protocols with minor modifications due to antibody optimization. Cells were fixed and co-labeled with antibody. The antibodies are listed in the Supplementary Tab. S1.

2.11. Lentiviral infection

The lentiviral expression vectors, including 4 in 1 Gipz-shTOPK, vehicle control Gipz-shMOCK and packaging vectors, including pMD2.0G and psPAX2, were purchased from VigeneBioscience. Inc. To prepare TOPK viral particles, each viral vector and packaging vectors (pMD2.0G and psPAX2) were transfected into HEK293T cells using PEI following the manufacturer's suggested protocols. The transfection medium was changed at 6 h after transfection and then cells were cultured for 36–72 h. The viral particles were harvested by filtration using a 0.45-μm syringe filter, then combined with 8 μg/mL of ADV-HR (lentivirus coinfection regent, Vigene Bioscience) and infected into 60% confluent colorectal cells overnight. The cell culture medium was replaced with fresh complete growth medium for 24 h and then cells were selected with puromycin (1.5 μg/mL) for 36 h. The selected cells were used for experiments.

2.12. Xenograft mouse model

All animal experiments have been approved by the Institutional Animal Care and Treatment Committee of Sichuan University in China (Permit Number: 20170135) and were carried out in accordance with the approved guidelines. BALB/c nude mice (6- to 9-week-old) used in this study were obtained from Beijing HFK bioscience CO. LTD, Beijing, China and were maintained in a specific-pathogen-free (SPF) condition facility. Mouse injected subcutaneously with $\sim 1 \times 10^7$ CRC cells were randomly divided into three groups when tumor volumes were around 100 mm^3: (i) untreated control group; (ii) 10 mg SKLB-C05/kg of body weight; (iii) 20 mg/kg SKLB-C05/kg of body weight. SKLB-C05 or the control consisting of 2.5% DMSO in normal saline (NS) solution was administered at the indicated doses once a day for 21 days by oral gavage. Two diameters of the individual tumor were measured by electronic slide caliper every three days. Tumor volume was calculated using the following formula: tumor volume (mm^3) = 0.52 × length × $width^2$. Mice were monitored for 21 days, at which time mice were euthanized and tumors and organs were extracted. The TGI values were calculated with the following formula: $TGI = [1-(T_n-T_0)/(C_n-C_0)] \times 100\%$, T_0 and T_n represent average tumor volume before treatment and that of n days after treatment in SKLB-C05-treated group. C_0 and C_n represent average tumor volume before treatment and that of n days after treatment in vehicle control group, in this assay, n is 21st day.

2.13. Hepatic metastasis model

Balb/c nude mice were anesthetized using an i.p. injection of a chloral hydrate solution. Under aseptic conditions, a small longitudinal incision was made in the left upper flank to visualize the spleen, and 5×10^6 HCT116 cells in 100 μL of medium (FBS and antibiotic free) were injected under the spleen capsule. Then animals were randomly divided into three groups and treated with indicated dose of SKLB-C05 or control once daily by oral gavage. Animals were sacrificed at 28 days, and livers were isolated at that time. After photographs were taken, livers were fixed in 10% buffered formalin and paraffin-embedded. Tumors were enumerated by visual inspection and liver sections were stained with H&E and also subjected to IHC.

2.14. Pharmacokinetic analysis

For the pharmacokinetic analysis, blood from Sprague-Dawley rats dosed with SKLB-C05 was collected in pre-chilled K^2-ethylenediaminetetraacetic acid (EDTA) tubes at pre-specified time intervals. The plasma samples were isolated by centrifugation, and the concentrations of SKLB-C05 were determined using LC-MS/MS. The compound was dissolved in NS consisting of 2.5% DMSO.

2.15. Statistical analysis

All quantitative results are expressed as mean values ± SD. Statistically significant differences were obtained using the Student's *t*-test. $P < 0.05$ was considered to be statistically significant.

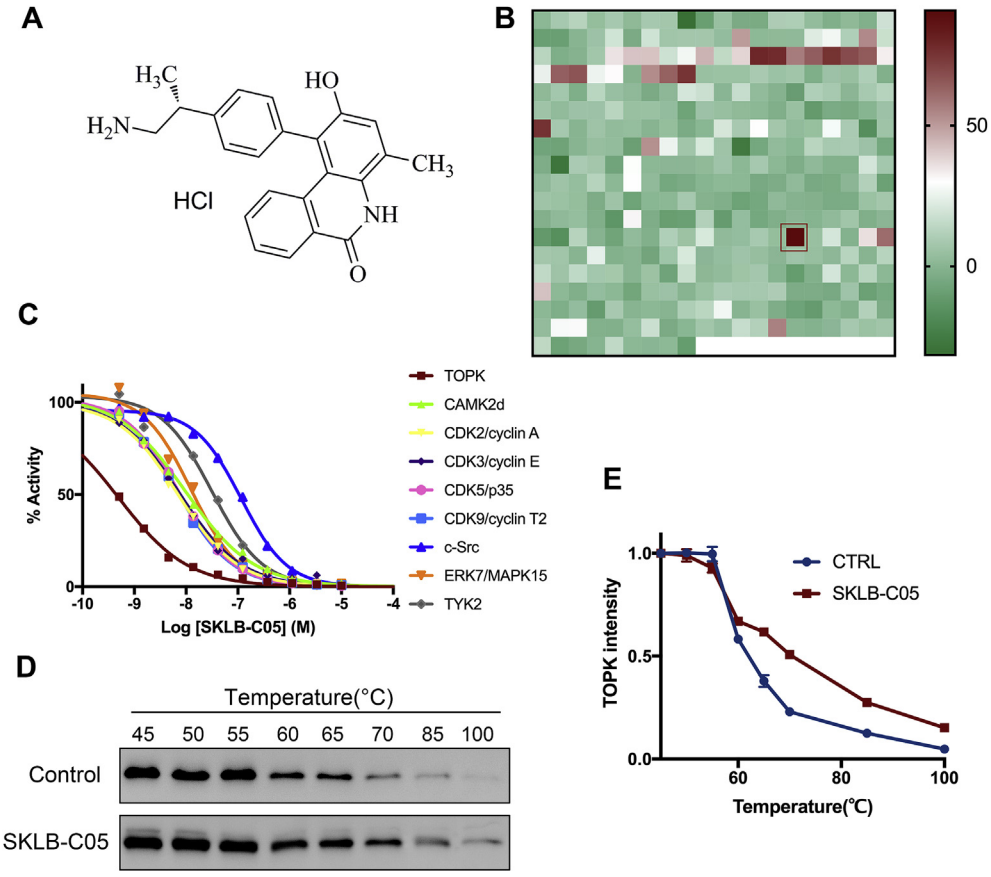

Fig. 1. SKLB-C05 is a selective TOPK inhibitor. (A) Chemical structure of SKLB-C05 (B) Heat map showing inhibitory rate against activities of 369 kinds of kinases. The diamond in the red frame represents TOPK. (C) Potency of SKLB-C05 against 9 kinds of kinases activity. (D) (E) Cellular thermal shift assay from 45 to 100 °C of HCT116 lysates with or without SKLB-C05 incubation. The image in immunoblotting are exhibited and graphic data run in triplicated are shown as mean ± SEM. (For interpretation of the references to color in this figure legend, the reader is referred to the Web version of this article.)

3. Results

3.1. Development of SKLB-C05

We identified the potent TOPK inhibitor SKLB-C05 (Fig. 1A) and *in vitro* kinase assays revealed its excellent inhibition of TOPK kinase with a median-inhibitory concentration (IC_{50}) of 0.5 nM. To confirm the specificity of SKLB-C05, its activity against 369 human kinases was measured at a concentration of 0.05 μM. The result showed that the inhibition ratio of SKLB-C05 against most of the kinases tested was minimal, whereas numerous kinases displayed an inhibition ratio above 50% (Fig. 1B, Supplementary Tab. S2). Thus, the IC_{50} of SKLB-C05 against these kinases were tested, and there is an over 10 times disparity of IC_{50} between TOPK and eight other kinases tested (Fig. 1C, Supplementary Tab. S3). To investigate whether SKLB-C05 would combine with TOPK protein *in vitro*, we conducted thermal shift assay in HCT116 cell line and as shown in Fig. 1D and E, SKLB-C05 increased the thermal stability of TOPK, with a temperature shift of approximately 5 °C, indicating a combination of SKLB-C05 and TOPK protein. These results illustrated that SKLB-C05 specifically inhibited TOPK.

To determine the properties of compound, the solubility of SKLB-C05 in six solvent and Log $D_{7.4}$ between water and n-caprylic alcohol were tested, and the results are shown in Supplementary Tab. S4. From the results, we conclude that SKLB-C05 can be well dissolved in both lipid and aqueous solution, and a log D value of 1.62 is beneficial for its bioavailability.

3.2. SKLB-C05 inhibited TOPK-positive CRC cell growth and migration and induced apoptosis

To evaluate the anticancer activity of SKLB-C05 on CRC cells, HCT116, SW480, SW620, and DLD-1 cell lines were exposed to graded concentrations of SKLB-C05 (3.91, 7.81, 15.63, 31.25, 62.5, 125, 250, 500, and 1000 nM) for 24, 48, and 72 h, and the cell viability index was calculated relative to the untreated control cells. The results showed that treatment with SKLB-C05 for 48 and 72 h but not 24 h lead to a significant decrease of active CRC cells (Fig. 2A). Colony formation assays showed that treatment of HCT116, SW480, DLD-1, and SW620 cells with SKLB-C05 significantly reduced the colony number and size in a concentration-dependent manner ($p < 0.05$, Fig. 2B, Supplementary Fig. S1A). Furthermore, FCM analysis showed an increase in the population of apoptotic cells (Annexin V-positive) with increasing concentrations of SKLB-C05 (Fig. 2C). IF staining also showed that exposure of HCT116, SW480, and DLD-1 cells to SKLB-C05 for 48 h significantly decreased the cell number and induced nuclear fragmentation, cell shrinkage, and formation of condensed nuclei with bright-blue fluorescence (arrows, Supplementary Fig. S1C), suggesting that SKLB-C05 efficiently induced apoptosis.

In the wound healing assay, the scratch created in the SKLB-C05-treated cell culture healed slower than that in the untreated cell culture did (Fig. 2D). The Transwell assay indicated that after exposure to SKLB-C05 for 24 h, fewer CRC cells penetrated the matrigel than those in the untreated control group (Fig. 2E). In summary, these results demonstrated that SKLB-C05 suppressed the migration and invasion capacity of CRC cells.

These data all indicate that SKLB-C05 exhibited potential anti-tumorigenic effects in CRC cells.

3.3. Inhibition of CRC cell proliferation by SKLB-C05 is TOPK-dependent

To verify if SKLB-C05's anti-tumorigenic effect is mediated by targeted inhibition of TOPK, we examined the sensitivity of a panel of CRC cells (human colon cancer HCT116, SW620, caco2, SW480, LOVO, HT-29, colo205, HCT-15, DLD-1, and human rectum cancer SW837 cells) to SKLB-C05 using the MTT method. Furthermore, the expression of TOPK in these cells was also examined using immunoblotting method. As

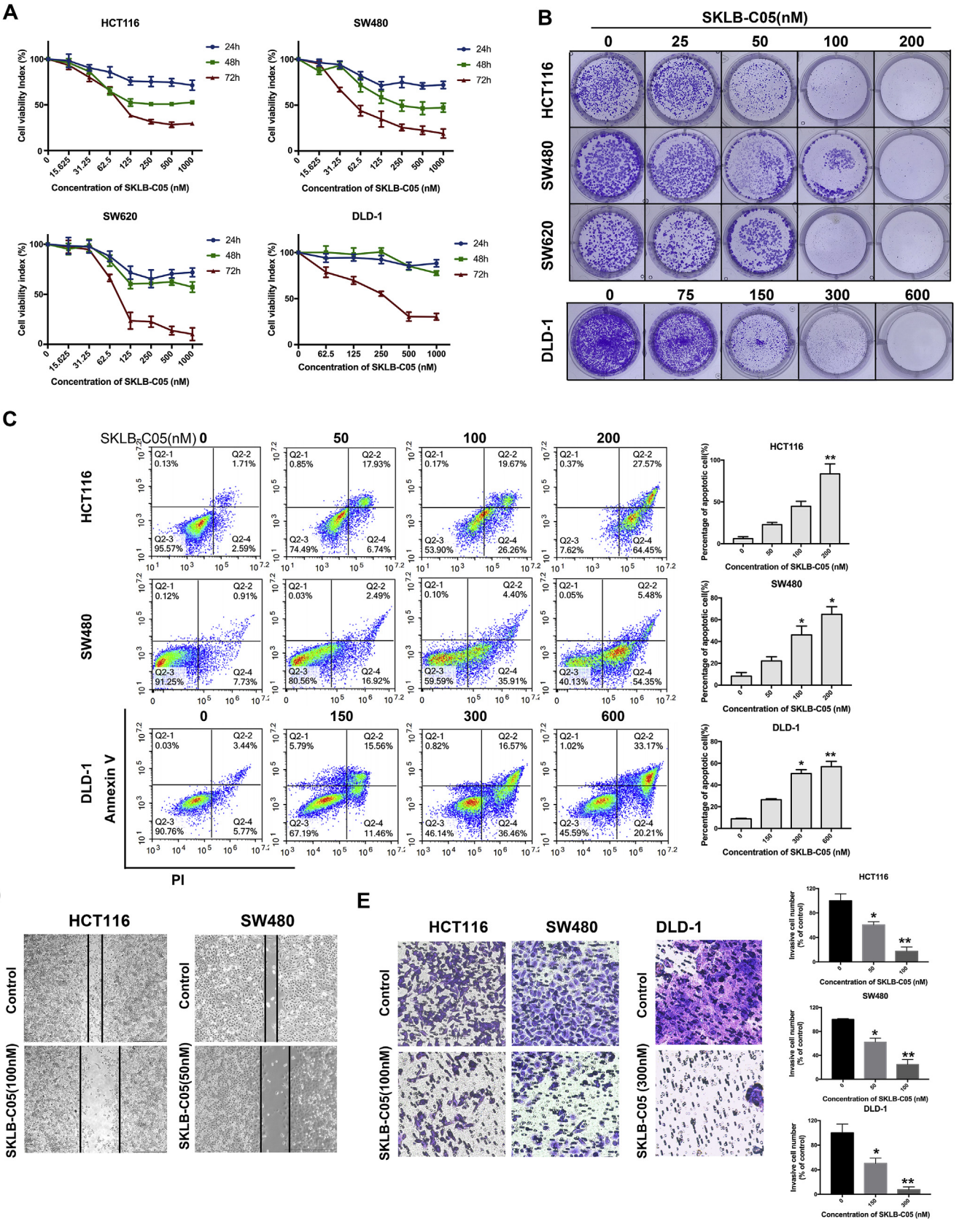

(caption on next page)

Fig. 2. SKLB-C05 suppressed proliferation, migration and invasion of CRC cell and induced cell apoptosis. (A) HCT116, SW480, DLD-1, SW620 cell lines were treated with increasing dose of SKLB-C05 for 24 h, 48 h and 72 h, respectively. The graphic data shown are mean ± SD from 3 independent experiments. The cell viability indexes were the percentage of cells contrast to DMSO-treated group at respect time. (B) Effects of SKLB-C05 on cell colony formation after treated by SKLB-C05 for two weeks. (C) FCM analysis of Annexin V/PI staining CRC cell lines after SKLB-C05 treatment for 48 h, quantification was shown in the right panel, *p < 0.05, **p < 0.01 vs vehicle control. (D) SKLB-C05 decreased CRC cell migration *in vitro*. HCT116 and SW480 colon cancer cells were subjected to a wound healing assay. Photographs were taken when cells were treated with SKLB-C05 or vehicle control for 24 h after scratching (20 ×). Experiments were repeated twice. (B) SKLB-C05 decreased CRC cell invasion in transwell assay. HCT116, SW480 and DLD-1 cells were planted in the upper chamber membrane which were pre-treated with matrigel and photographs were taken after treated with indicated dose of SKLB-C05 for 48 h (20 ×). Invading cells were counted from five random fields and experiments were repeated twice (right panel), *p < 0.05, **p < 0.01 vs vehicle control.

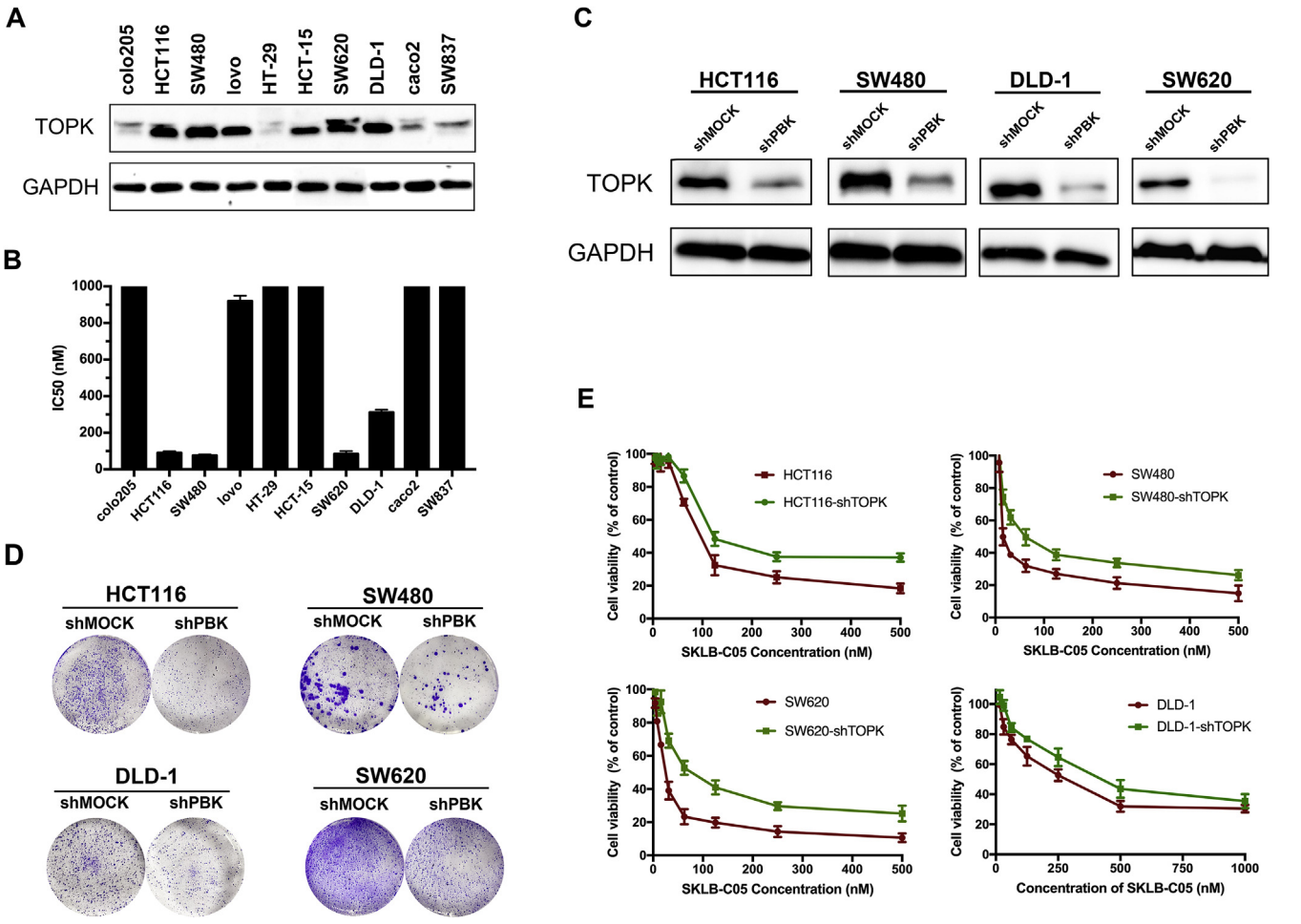

Fig. 3. SKLB-C05 selectively inhibited proliferation of TOPK-positive CRC cells. (A) Western blots show expression of TOPK in 10 CRC cell lines. (B) Graph indicates IC_{50} values of SKLB-C05 in these cell lines. (C) Immunoblotting analysis of efficiency of TOPK knockdown by shRNA in HCT116, SW480, SW620 and DLD-1 cells (D) Colony formation of parental and TOPK-deficiency HCT116, SW480, SW620 and DLD-1 cells (E) Sensitivity of CRC cells transfected with shMock or shTOPK to SKLB-C05 exposure. Cells were treated by SKLB-C05 for 72 h. Each experiment was repeated thrice.

shown in Fig. 3A, TOPK was relatively highly expressed in HCT116, SW480, DLD-1, and SW620 but not SW837, colo205, caco2, and especially HT-29 cell lines. Moreover, SKLB-C05 also exhibited markedly prioritized inhibitory activity on TOPK-positive CRC cells than TOPK-negative cells. Treatment with SKLB-C05 for 72 h showed IC_{50} values against HCT116, SW620, SW480, and DLD-1 cells of 96.17, 72.13, 80.39, and 320.90 nM, respectively (Fig. 3A), while values against the other cell lines were both above 1 μM. Besides, SKLB-C05 exhibited an over 10 times selective inhibitory rate on HCT116, SW480 and SW620 than non-cancer cell line Vero, the IC_{50} of SKLB-C05 against which is over 1 μM (Supplementary Fig. S1B).

Knockdown of PBK/TOPK in CRC cells using lentiviral short hairpin RNA (shRNA) vectors obviously reduced the protein level of TOPK and decreased the cell growth compared with that of the shMOCK group (Fig. 3B and C). Exposure of shTOPK and shMOCK cells to different concentrations of SKLB-C05 for 72 h revealed that shTOPK cell lines were obviously less sensitive to SKLB-C05 treatment than the parental cell lines were (Fig. 2D). This observation indicated that the TOPK-knockdown CRC cells acquired resistance to SKLB-C05 treatment. These results confirmed that TOPK played a critical role in CRC cell proliferation and, more importantly, the anti-proliferative effect of SKLB-C05 on CRC cells was largely TOPK-dependent.

3.4. SKLB-C05 inhibited TOPK and downstream target activation in human CRC cells

Evidence has indicated that hyperactivation of TOPK upregulates MAPK pathway molecules and further induces uncontrolled cell proliferation [13,39]. To determine the molecular mechanism of the anti-proliferative and apoptotic induction effect of SKLB-C05, we investigated its effect on TOPK-related signaling pathways in CRC cells. As shown in Fig. 4A, we detected an obvious concentration-dependent

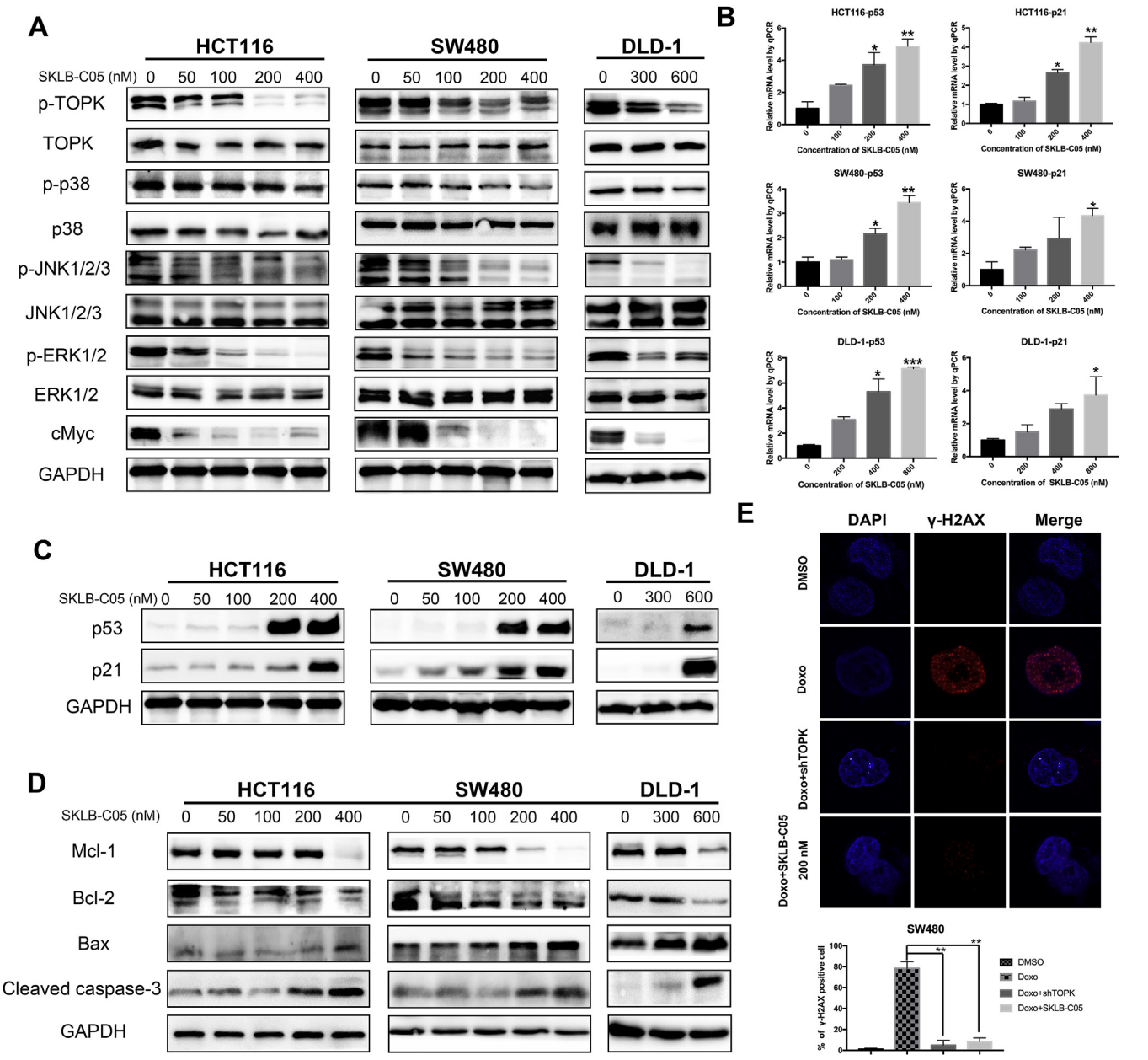

Fig. 4. SKLB-C05 inhibited TOPK downstream signaling. (A) Immunoblotting analyses of TOPK downstream MAPK pathway protein after treated by SKLB-C05 for 48 h. Each has the expression of GAPDH as the internal control. (B) mRNA level of p53 and p21 determined by qRT-PCR after treated by SKLB-C05 for 48 h. Values are mean ± SD (n = 3), *p < 0.05, **p < 0.01, ***p < 0.001 vs vehicle control. (C) p53 and p21 protein level determined by immunoblotting after treated by SKLB-C05 for 48 h. (D) Immunoblotting analyses of apoptosis cascade related protein level, including JNK targeted Mcl-1, and Bcl-2, Bax and cleaved caspase-3, after treated by SKLB-C05 for 48 h. (E) Parental and TOPK-deficiency SW480 cells were exposure to DMSO or doxorubicin (0.1 μg/mL) for 4 h and then treated by SKLB-C05 (200 nM) or vehicle control for 24 h. The γ-H2AX foci were analyzed by immunofluorescence microscopy. The quantification of γ-H2AX positive cells (≥5 foci) was in the bottom panel, **p < 0.01.

decrease in the expression of phosphorylated TOPK (p-TOPK) at Thr9 following SKLB-C05 treatment, without a change in the total TOPK protein level, consistent with previous results in the kinase assay. We also found that SKLB-C05 treatment markedly downregulated the expression of p-ERK1/2, p-p38 and p-JNK1/2/3, without changing the global expression of ERK1/2 and JNK1/2/3. Our results suggested that SKLB-C05 suppressed TOPK kinase activity, and then blocked the phosphorylation of ERK1/2, p38, and JNKs, which are the downstream factors of TOPK. Reports indicated that cMyc can be stabilized by Ras/MAPK pathway activation, and ERK1/2 can phosphorylate Ser62 of Myc and enhance its stability [40,41], so we further investigated whether the inhibition of MAPK pathway would influence the stability of cMyc protein. The results showed that SKLB-C05 significantly downregulated c-Myc protein levels, which likely mediated its suppression of cell proliferation and induced apoptosis (Fig. 4A).

A previous study verified that TOPK inhibited p53 and its downstream target [11], so we inferred that the suppression of TOPK by SKLB-C05 might rescue p53 and its downstream target. Therefore, qRT-PCR analysis was performed in HCT116, SW480, and DLD-1 cells after treatment with different concentrations of SKLB-C05 for 48 h. As shown in Fig. 4B, mRNA quantitation of p53 and p21 in SKLB-C05-treated groups significantly increased compared with control groups. Consistent with this result, the protein levels of p53 and p21 were also highly induced by increasing concentrations of SKLB-C05 (Fig. 4C), indicating that SKLB-C05 activated p53 by inhibiting TOPK, which contributed to inducing apoptosis.

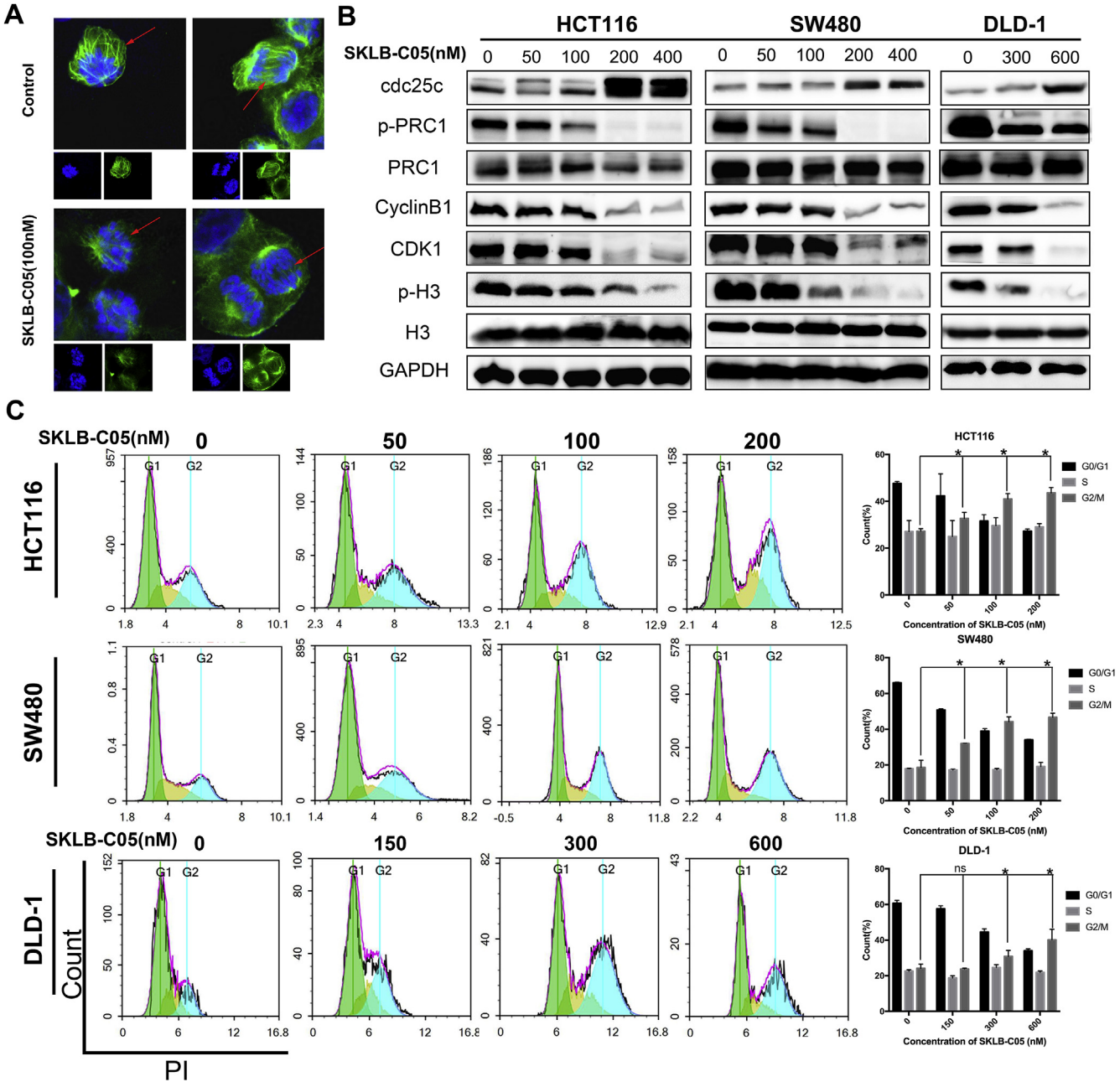

Fig. 5. Influence of SKLB-C05 on mitosis. (A) HCT116 cells were synchronized by thymine for 16 h and treated with 100 nM SKLB-C05 or DMSO for 16–24 h, the spindles were determined by immunostaining with α-tubulin (green), and DNA was marked by DAPI (blue), the main images show merged picture, and the insets show respect staining with DAPI (blue) and α-tubulin (green). (B) Immunoblotting analyses of key mitotic related protein after treated by SKLB-C05 for 48 h. (C) HCT116, SW480 and DLD-1 cells were treated with indicated concentration of SKLB-C05 for 48 h, and then cell-cycle distribution was analyzed by flow cytometry (FCM). Percentages of the cell cycle are presented at the right panel. Values are mean ± SD (n = 3); ns, not statistically significant, *P < 0.05, vs. vehicle control. (For interpretation of the references to color in this figure legend, the reader is referred to the Web version of this article.)

Our immunoblotting analyses also indicated that SKLB-C05 accelerated apoptosis by targeting members of the Bcl-2 family, including Mcl-1, Bcl-2, and Bax, and triggered the caspase-regulated cascade (Fig. 4D). In addition, activation of H2AX contributes to DNA damage reparations and previous studies have reported that suppression of TOPK by shRNA inhibited the activation of H2AX through inhibition of p38 activation [9]. In our study, SKLB-C05 treatment for 24 h markedly inhibited the expression of γ-H2AX activated by exposure to doxorubicin (Fig. 4E). Taken together, these results suggested that SKLB-C05 accelerated apoptosis relevant signaling and inhibited DNA self-reparations in CRC cells.

3.5. SKLB-C05 disturbed spindle during mitosis and induced cell accumulation in G2/M phase

TOPK was initially identified as a mitotic protein kinase [4], and accumulating reports have focused on the critical roles of TOPK in cancer cell mitosis. When TOPK expression was suppressed, formation of spindle midzone was thinned and dimmed and cytokinesis was disturbed, which likely deserve to a block of the function of TOPK/cyclinB1/CDK1 complex [42]. We performed IF imaging to observe the nuclei and tubulin during the mid-term phase of mitosis after treatment with or without (control) SKLB-C05. As shown in Fig. 5A, the spindle midzone was dimmed in SKLB-C05-treated HCT116 cells in contrast to

the control cells.

Studies indicate that disturbing TOPK functions contributes to disrupting the uncontrolled cell cycle [8,33]. Cell cycle progression is regulated by various cyclins, CDKs and CDK inhibitors (CKI). TOPK was reported to enhance the activity of cyclinB1/CDK1 in promoting cytokinesis by phosphorylating PRC1 [7]. Moreover, p21, which acts as a CKI, binds to and inhibits the activity of cyclinB1/CDK1 [43]. Therefore, we detected the cellular protein levels of these regulating factors. As shown in Fig. 5B, after treatment with SKLB-C05 for 48 h, the expressions of cyclinB1 and CDK1 were both inhibited. Furthermore, the expression of p-PRC1 and histone H3 were also downregulated while that of cdc25c was upregulated (Fig. 5B), indicating mitosis progression was blocked.

Cytokinetic failure, leading by inhibition of spindle formation in the midterm stage of mitosis, may increase cell distribution in G2/M phase in TOPK-inhibited cells. We conducted FCM analysis of SKLB-C05-treated cells and discovered that the cell cycle distribution was transformed, and a substantial accumulation of cells in G2/M phase was detected after exposure to SKLB-C05 for 48 h. The percentage of cells in G2/M phase rose with increasing concentrations of SKLB-C05 compared with control group, while cells in G0/G1 and S phases decreased (Fig. 5C).

These results confirmed that SKLB-C05 exhibited anti-proliferative activity by directly inhibiting TOPK function.

3.6. In vivo efficacy of SKLB-C05

Pharmacokinetic assays were conducted in SD rat to evaluate the compound circulation *in vivo*. The result showed that 20 mg/kg oral administration of SKLB-C05 was rapidly absorbed with a maximum concentration (C_{max}), mean residence time, and elimination half-life ($t_{1/2}$) of 8800 ng/mL, 3.29 h, and 4.36 h in rats. In addition, the > 100% oral bioavailability compared to that following intravenous injection proved that SKLB-C05 could be well absorbed in the gastrointestinal tract (Supplementary Table 5 and Fig. S2). This finding suggested that oral administration of 20 mg/kg is suitable for treatment.

We investigated the *in vivo* antitumor effect of SKLB-C05 in xenograft models of HCT116, SW480, and DLD-1 cells. The results showed that oral administration of 10 and 20 mg kg^{-1} SKLB-C05 once daily for 3 weeks showed TGI values of 64.3 and 92.4% in the HCT116 xenograft model, 54.2 and 88.9% in the SW480 xenograft model, and 46.3 and 67.5% in the DLD-1 xenograft model on day 21, respectively (Fig. 6A). Furthermore, a significant tumor weight slide was also observed (Fig. 6B). In addition, we observed no hematopoietic toxicity and pathological changes of main organs but there was a mild decrease in body weight compared with the vehicle-treated group (Supplementary Fig. S3A, B, C, and F), suggesting the mice were tolerant to SKLB-C05 treatment. To validate the results of the *in vivo* assays, we investigated the expression of downstream targets of TOPK proliferation, migration, and apoptosis markers using immunoblotting and IHC analyses of the CRC tumor samples. The p-H3 and p-ERK1/2-positive area of the IHC staining was markedly decreased in the SKLB-C05-treated groups. The Ki-67-positive cells (proliferative) declined, whereas the cleaved caspase-3 positive cells increased (Fig. 6C, Supplementary Fig. S3E). Furthermore, the immunoblotting results showed that the expression of p21 was strongly induced, and phosphorylated but not total histone H3, ERK1/2, p38, and JNK1/2/3 was markedly inhibited in the SKLB-C05-treated group (Fig. 6D). We also detected a decrease in phosphorylated FAK and MMP9, even a decrease of total FAK. Overall, these findings suggested that SKLB-C05 blocked proliferation and metastasis of human CRC by regulating specific TOPK downstream signaling.

3.7. SKLB-C05 blocked FAK/Src medicated migration-related signaling and inhibited hepatic metastasis of HCT116 model

Our cellular results indicated that SKLB-C05 markedly suppressed CRC cells migration and invasion. To mechanistically expound and confirm this discovery, we determined the protein expression correlated with cell migration and invasion using TOPK shRNA and SKLB-C05 treatment. Our data showed that the protein level of TOPK, p-ERK1/2, and p-H3 in the shTOPK group were decreased compared with the control group, confirming knocking-down efficacy of shRNA. The results also showed downregulation of p-Src, p-FAK, and MMP9 in TOPK-knockdown HCT116 and SW480 cell lines. (Fig. 7A), suggesting that inhibition of TOPK significantly blocked the activation of FAK-MMPs pathway. Furthermore, similar result was also observed in the SKLB-C05-treated group where both FAK, p-FAK, Src, p-Src, MMP9, and MMP2 were down-regulated in HCT116, SW480, and DLD-1 cells (Fig. 7B). This finding suggested that SKLB-C05 suppressed migration and invasion of CRC cells by blocking the Src/FAK-related migration signaling pathway by targeting TOPK.

We investigated the effect of SKLB-C05 on CRC metastasis in HCT116 hepatic metastasis mouse model. Cells were injected into the spleen of Balb/c nude mice, and indicated doses of SKLB-C05 were administrated by oral gavage 1 week after inoculation. After 28 days, the mice were euthanized and the livers were excised to evaluate metastasis. There was no obvious decline in body weight during treatment (Fig. 7E). The liver nodal metastasis found in mice in the 5 mg kg^{-1}·day^{-1} SKLB-C05-treated group was significantly decreased compared to that in the vehicle group, while nearly no metastatic tubercles were found in the 10 mg kg^{-1}·day^{-1} SKLB-C05-treated group. Representative liver metastases (arrows) and quantification (Fig. 7C and D) are shown. H&E and IHC staining showed that the tumor area and amount of Ki-67 were both markedly decreased with SKLB-C05 treatment (Fig. 7F and G), indicating that SKLB-C05 validly suppressed hepatic metastasis of CRC.

4. Discussion

TOPK, firstly discovered in lymphokine-activated killer T cells (T-LAK), is a member of MAPKK family. Abnormal expression of TOPK in colorectal and other cancers triggers excessive activation of a series of signaling pathways, such as the ERK1/2, p38, c-Jun, and NF (nuclear factor)- κB pathways [29,39,44] and, thus, correlated with proliferation, inflammation, and metastasis of tumor cells. TOPK was regarded as one of the most valuable biomarker in colon carcinoma and, so, studies targeting this molecule as a therapeutic strategy are worth conducting [45]. To date, there is no TOPK-targeted inhibitor under clinical trials or coming into the market. However, some potential TOPK inhibitors including HI-TOPK-032, OTS514, OTS964, and ADA-07 have been reported, but the discovery of specific and highly active inhibitors with novel structures is still necessary.

In our present study, a novel, potential TOPK selective inhibitor SKLB-C05 was demonstrated. Concordantly with previous reports, inhibition of TOPK activity by SKLB-C05 attenuated the malignant proliferation and metastatic phenotype associated with aberrant expression of TOPK in CRC. One of the most highlighted actions of SKLB-C05 is its suppression of TOPK activity with an IC_{50} of 0.5 nM *in vitro*, which is considerably lower than the simultaneously measured values of OTS514 and OTS964 (10.7 and 353.7 nM, respectively). Moreover, SKLB-C05 also exhibited a prominent antitumorigenic activity on CRC, and its anti-proliferative effect was TOPK- dependent—— knockdown of TOPK rendered the CRC cells less sensitive to SKLB-C05 treatment than the parental cell lines were. More importantly, we found that TOPK promote metastasis via FAK/Src-MMP signaling, and knockdown of TOPK or its inhibition by SKLB-C05 downregulated FAK, Src, MMP2, and MMP9 and inhibited CRC metastasis *in vitro* and *in vivo*.

TOPK is an upstream kinase of p38 and JNKs, which are subgroups of the MAPK family, and at the same time, TOPK phosphorylate ERK1/2, too [39]. We found that the expression levels of p-ERK1/2, p-p38, and p-JNK1/2/3 were inhibited by SKLB-C05 treatment in HCT116, SW480, and DLD-1 cells, which further regulated their downstream

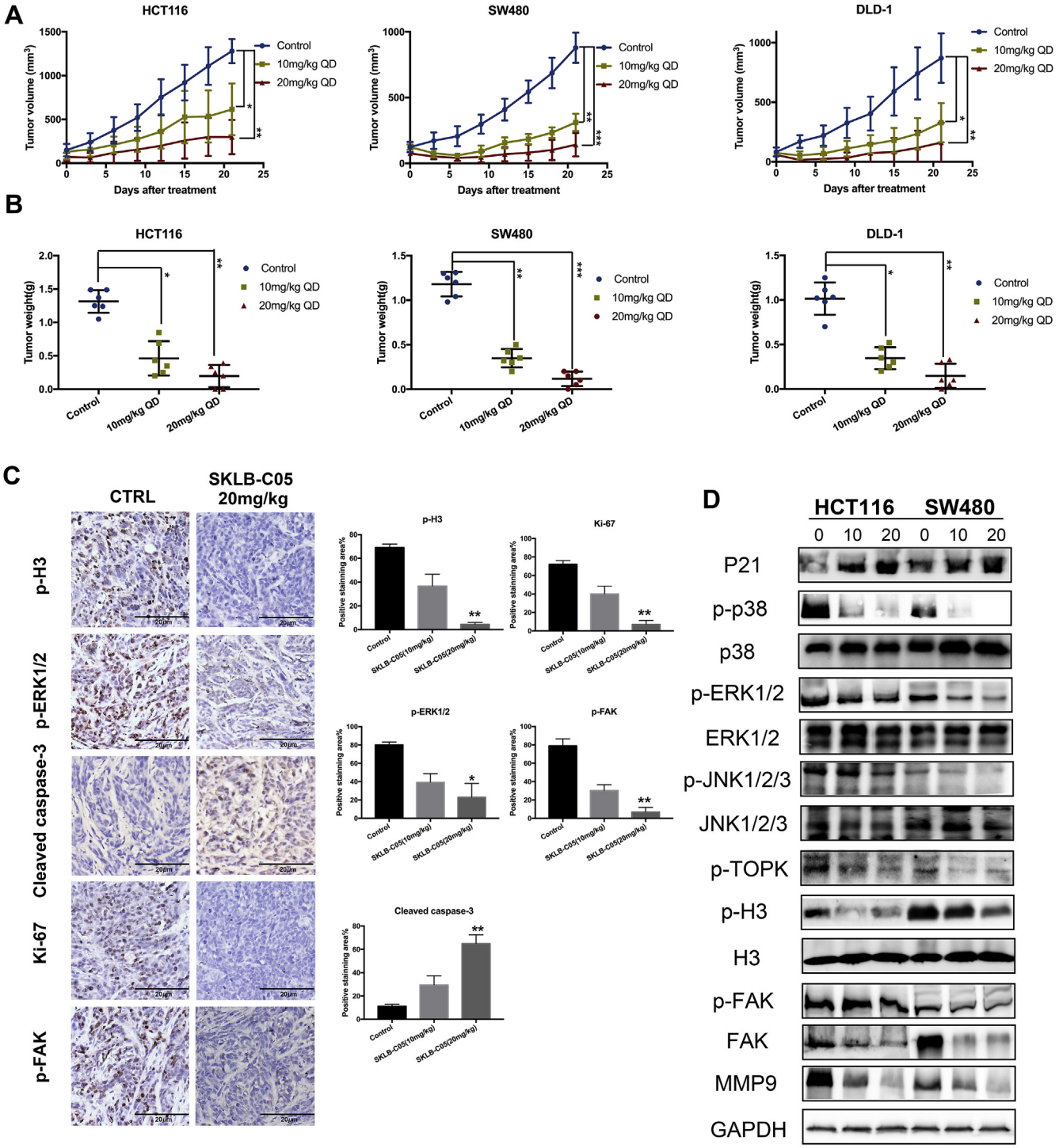

Fig. 6. *In-vivo* efficacy of SKLB-C05 in CRC xenograft models. Nude mice bearing HCT116 (left panel), SW480 (middle panel) or DLD-1 (right panel) (n = 6) were orally treated with vehicle control or SKLB-C05 once every day for 3 weeks. Mean tumor volumes ± SD (A) and weight of tumors from sacrificed mice (Horizontal lines represent the means ± SD) (B) are shown, *p < 0.05, **p < 0.01, ***p < 0.001. (C) Tumor tissues from HCT116 xenograft treated with vehicle control, SKLB-C05 (10 mg/kg) or SKLB-C05 (20 mg/kg) for 21 days were immunohistochemically analyzed with anti-p-ERK1/2, anti-p-histone H3, anti-Ki-67, anti-cleaved caspase-3 and anti-p-FAK antibodies (n = 3). Representative images and quantitative analysis of percentage of positive staining are shown. *P < 0.05, **p < 0.01. (D) SKLB-C05 inhibits TOPK-target protein expression in HCT-116 colon tumor tissues. The tumor tissues from groups treated with vehicle control, 10 mg or 20 mg/kg SKLB-C05 per body weight were immunoblotted with antibodies to detect p-TOPK, total histone H3, p-histone H3, p-ERK1/2, p-p38, p-JNK1/2, p21, p-FAK and MMP9. GAPDH was used to verify equivalent loading of protein.

signaling such as cMyc and H2AX, leading to apoptosis and the failure of DNA damage reparation of CRC cells. The expression of p53 and its downstream target p21 was highly induced through inhibition of TOPK by SKLB-C05. As a mitosis relevant kinase, over-expressed TOPK promote uncontrolled cell cycle and mitosis progression in tumor cells [4,7]. In this study, we discovered that SKLB-C05 disturbed the formation of spindles in the midterm stage of mitosis, and blocked CRC cell cycle progression along with suppression of the cyclinB1/CDK1 complex and p-histone H3.

In xenograft mouse models, SKLB-C05 optimally suppressed

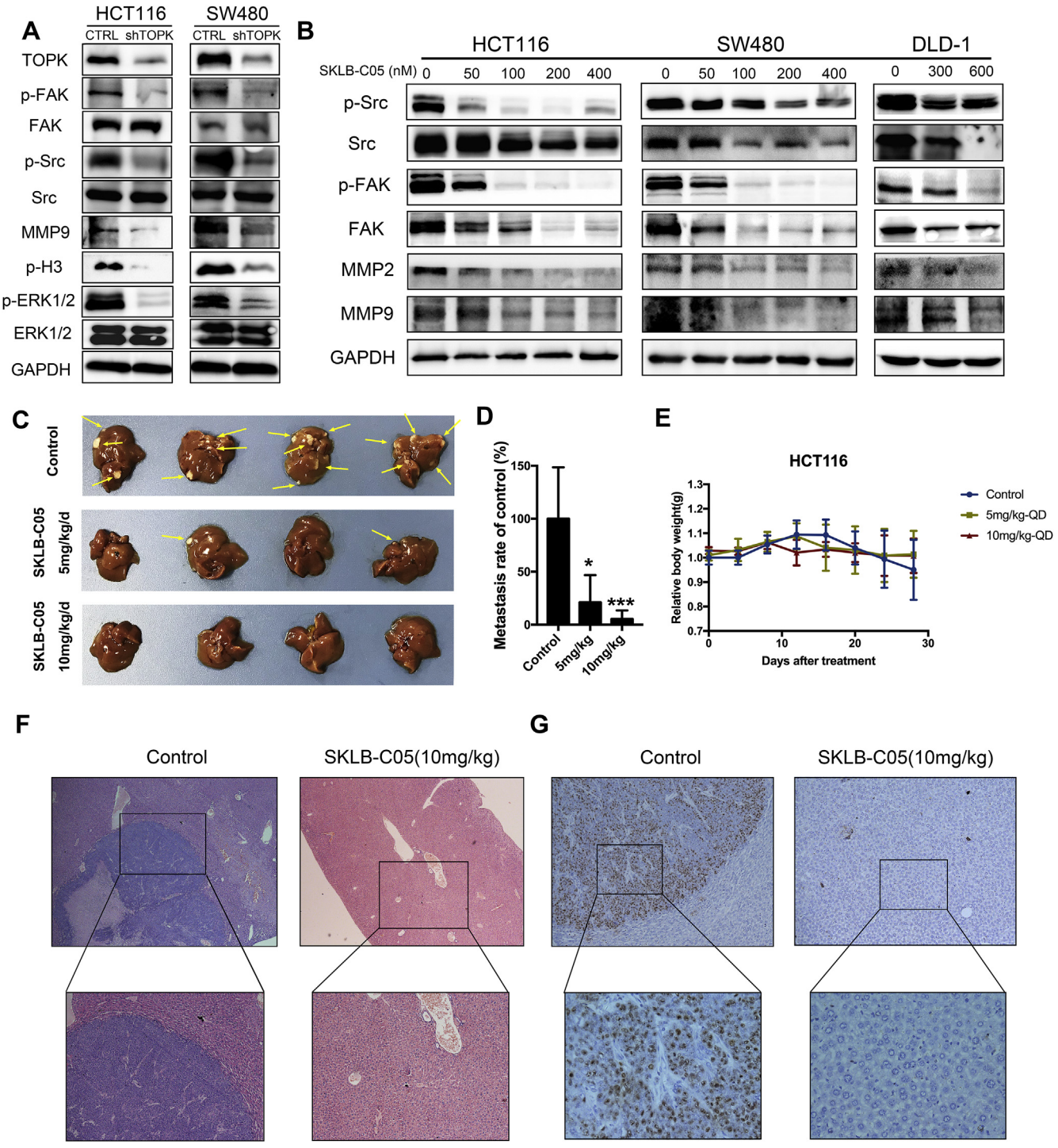

Fig. 7. SKLB-C05 exhibited inhibitory effect on HCT116 hepatic metastasis (A) Immunoblotting analysis of parental (CTRL) and TOPK-deficiency (shTOPK) HCT116 and SW480 cells, including the expressions of p-FAK, MMP9, p-ERK1/2 and p-H3. GAPDH was used to verify equal protein loading (B) Immunoblotting analysis of HCT116 and SW480 cells following SKLB-C05 treatment, including the expressions of p-Src, FAK/p-FAK, MMP2 and MMP9. GAPDH was used to verify equal protein loading. (C) Metastasis (arrows) shown of representative mouse per group at the 30_{th} days after injection of HCT116 cells, and (D) quantification of the amount of node of liver metastasis, *$p < 0.05$, ***$p < 0.001$. (E) Data showing average body weight changes of the control, SKLB-C05 (5 mg/kg) and SKLB-C05 (10 mg/kg) treated mice in xenograft model ($n = 6$). Points, mean value; bars, SD (F) H&E staining of non-metastatic and metastatic liver tissue (10 μm sections) of vehicle control and 10 mg/kg SKLB-C05 group is shown (2.5 × magnification). (G) Ki-67 staining of non-metastatic and metastatic liver tissue (10 μm sections) is shown (4 × magnification).

HCT116, SW480, and DLD-1 tumor growth at 20 mg kg^{-1} with once daily dosing for 21 days, and some tumors even regressed after short-term treatment. SKLB-C05 also potently inhibited hepatic metastasis in the HCT116 model.

In summary, we demonstrated a novel specific TOPK inhibitor, SKLB-C05, which exhibited excellent anti-tumorigenic activity on CRC. Importantly, SKLB-C05 displayed highly selectivity on TOPK kinase and antitumor and anti-metastasis activity at lower doses following oral administration. Taken together, our findings indicate that SKLB-C05 is a potential TOPK inhibitor that may be useful in treating a variety of

malignancies, especially CRC.

Conflicts of interest

The authors declare no potential conflicts of interest.

Authors' contributions

Tiantao Gao and Zhihao Liu designed the study, analyzed and interpretated the data and write, review or revise the manuscript, Xi Yu and Xuejiao Song revised the manuscript, Quanfang Hu offered the compound, Cuiting Peng, Ying Xu, Jun Zeng and Weiqiong Zuo made efforts on acquisition of data and development of methodology, Xi Hu, Zhanzhan Feng and Hualong He helped to carry out some of the assays.

Acknowledgement

We thank Chunqi Liu for technological support during the course of this study, we also thank the AstaTech (Chengdu) BioPharmaceutical Corp for financial support.

Abbrevations

PI3K	phosphoinositide 3-kinase
PTEN	phosphatase and tensin homolog
FAK	focal adhesion kinase
Src	steroid receptor coactivator
MMP	matrix metalloproteinase
PRC1	protein regulator of cytokinesis 1
Bcl-2	B-cell lymphoma 2
Mcl-1	myeloid cell leukemia 1
Bax	Bcl-2-associated X protein
H2AX	H2A histone family member X
CDK	cyclin-dependent kinase
Log D	Log of the distribution coefficient:
MTT	Propidium Iodide: PI; 3-(4,5-dimethylthiazol-2-yl)-2,5-diphenyltetrazolium bromide
DMSO	dimethyl sulfoxide
PEI	polyetherimide
LC-MS	liquid chromatography-tandem mass spectrometry
H&E	Hematoxylin and eosin
TGI	tumor growth inhibition

Appendix A. Supplementary data

Supplementary data to this article can be found online at https://doi.org/10.1016/j.canlet.2018.12.016.

References

[1] J.D. Dougherty, A.D. Garcia, I. Nakano, M. Livingstone, B. Norris, R. Polakiewicz, E.M. Wexler, M.V. Sofroniew, H.I. Kornblum, D.H. Geschwind, PBK/TOPK, a proliferating neural progenitor-specific mitogen-activated protein kinase kinase, J. Neurosci. 25 (2005) 10773–10785.

[2] Y. Abe, S. Matsumoto, K. Kito, N. Ueda, Cloning and expression of a novel MAPKK-like protein kinase, lymphokine-activated killer T-cell-originated protein kinase, specifically expressed in the testis and activated lymphoid cells, J. Biol. Chem. 275 (2000) 21525–21531.

[3] D. Herrero-Martin, D. Osuna, J.L. Ordonez, V. Sevillano, A.S. Martins, C. Mackintosh, M. Campos, J. Madoz-Gurpide, A.P. Otero-Motta, G. Caballero, A.T. Amaral, D.H. Wai, Y. Braun, M. Eisenacher, K.L. Schaefer, C. Poremba, E. de Alava, Stable interference of EWS-FLI1 in an Ewing sarcoma cell line impairs IGF-1/IGF-1R signalling and reveals TOPK as a new target, Br. J. Canc. 101 (2009) 80–90.

[4] S. Gaudet, D. Branton, R.A. Lue, Characterization of PDZ-binding kinase, a mitotic kinase, Proc. Natl. Acad. Sci. U. S. A 97 (2000) 5167–5172.

[5] J.H. Park, M.L. Lin, T. Nishidate, Y. Nakamura, T. Katagiri, PDZ-binding kinase/T-LAK cell-originated protein kinase, a putative cancer/testis antigen with an oncogenic activity in breast cancer, Cancer Res. 66 (2006) 9186–9195.

[6] I. Elmaci, M.A. Altinoz, R. Sari, F.H. Bolukbasi, Phosphorylated Histone H3 (PHH3) as a Novel Cell Proliferation Marker and Prognosticator for Meningeal Tumors: a Short Review, Applied immunohistochemistry & molecular morphology: AIMM, 2017.

[7] J.H. Park, T. Nishidate, Y. Nakamura, T. Katagiri, Critical roles of T-LAK cell-originated protein kinase in cytokinesis, Cancer Sci. 101 (2010) 403–411.

[8] Y. Abe, T. Takeuchi, L. Kagawa-Miki, N. Ueda, K. Shigemoto, M. Yasukawa, K. Kito, A mitotic kinase TOPK enhances Cdk1/cyclin B1-dependent phosphorylation of PRC1 and promotes cytokinesis, J. Mol. Biol. 370 (2007) 231–245.

[9] V. Ayllon, R. O'Connor, PBK/TOPK promotes tumour cell proliferation through p38 MAPK activity and regulation of the DNA damage response, Oncogene 26 (2007) 3451–3461.

[10] S.M. Oh, F. Zhu, Y.Y. Cho, K.W. Lee, B.S. Kang, H.G. Kim, T. Zykova, A.M. Bode, Z. Dong, T-lymphokine-activated killer cell-originated protein kinase functions as a positive regulator of c-Jun-NH2-kinase 1 signaling and H-Ras-induced cell transformation, Cancer Res. 67 (2007) 5186–5194.

[11] F. Hu, R.B. Gartenhaus, D. Eichberg, Z. Liu, H.B. Fang, A.P. Rapoport, PBK/TOPK interacts with the DBD domain of tumor suppressor p53 and modulates expression of transcriptional targets including p21, Oncogene 29 (2010) 5464–5474.

[12] T.A. Zykova, F. Zhu, T.I. Vakorina, J. Zhang, L.A. Higgins, D.V. Urusova, A.M. Bode, Z. Dong, T-LAK cell-originated protein kinase (TOPK) phosphorylation of Prx1 at Ser-32 prevents UVB-induced apoptosis in RPMI7951 melanoma cells through the regulation of Prx1 peroxidase activity, J. Biol. Chem. 285 (2010) 29138–29146.

[13] S. Li, F. Zhu, T. Zykova, M.O. Kim, Y.Y. Cho, A.M. Bode, C. Peng, W. Ma, A. Carper, A. Langfald, Z. Dong, T-LAK cell-originated protein kinase (TOPK) phosphorylation of MKP1 protein prevents solar ultraviolet light-induced inflammation through inhibition of the p38 protein signaling pathway, J. Biol. Chem. 286 (2011) 29601–29609.

[14] I. Zlobec, M. Molinari F Fau - Kovac, M.P. Kovac M Fau - Bihl, H.J. Bihl Mp Fau - Altermatt, J. Altermatt Hj Fau - Diebold, H. Diebold J Fau - Frick, M. Frick H Fau - Germer, M. Germer M Fau - Horcic, M. Horcic M Fau - Montani, G. Montani M Fau - Singer, H. Singer G Fau - Yurtsever, A. Yurtsever H Fau - Zettl, L. Zettl A Fau - Terracciano, L. Terracciano L Fau - Mazzucchelli, P. Mazzucchelli L Fau - Saletti, M. Saletti P Fau - Frattini, K. Frattini M Fau - Heinimann, A. Heinimann K Fau - Lugli, A. Lugli, Prognostic and Predictive Value of TOPK Stratified by KRAS and BRAF Gene Alterations in Sporadic, Hereditary and Metastatic Colorectal Cancer Patients.

[15] S.M. Oh, Y.-Y. Zhu F Fau - Cho, K.W. Cho Yy Fau - Lee, B.S. Lee Kw Fau - Kang, H.-G. Kang Bs Fau - Kim, T. Kim Hg Fau - Zykova, A.M. Zykova T Fau - Bode, Z. Bode Am Fau - Dong, Z. Dong, T-lymphokine-activated Killer Cell-originated Protein Kinase Functions as a Positive Regulator of C-Jun-NH2-kinase 1 Signaling and H-ras-induced Cell Transformation..

[16] T.A. Zykova, F. Zhu, L. Wang, H. Li, R. Bai, D.Y. Lim, K. Yao, A.M. Bode, Z. Dong, The T-LAK cell-originated protein kinase signal pathway promotes colorectal cancer metastasis, EBioMedicine 18 (2017) 73–82.

[17] O.L. PC, S.A. Penny, R.T. Dolan, C.M. Kelly, S.F. Madden, E. Rexhepaj, D.J. Brennan, A.H. McCann, F. Ponten, M. Uhlen, R. Zagozdzon, M.J. Duffy, M.R. Kell, K. Jirstrom, W.M. Gallagher, Systematic antibody generation and validation via tissue microarray technology leading to identification of a novel protein prognostic panel in breast cancer, BMC Canc. 13 (2013) 175.

[18] H. Sun, L. Zhang, C. Shi, P. Hu, W. Yan, Z. Wang, Q. Duan, F. Lu, L. Qin, T. Lu, J. Xiao, Y. Wang, F. Zhu, C. Shao, TOPK Is Highly Expressed in Circulating Tumor Cells, Enabling Metastasis of Prostate Cancer.

[19] M.C. Shih, J.Y. Chen, Y.C. Wu, Y.H. Jan, B.M. Yang, P.J. Lu, H.C. Cheng, M.S. Huang, C.J. Yang, M. Hsiao, J.M. Lai, TOPK/PBK promotes cell migration via modulation of the PI3K/PTEN/AKT pathway and is associated with poor prognosis in lung cancer, Oncogene 31 (2012) 2389–2400.

[20] F. He, Q. Yan, L. Fan, Y. Liu, J. Cui, J. Wang, L. Wang, Y. Wang, Z. Wang, Y. Guo, G. Huang, PBK/TOPK in the differential diagnosis of cholangiocarcinoma from hepatocellular carcinoma and its involvement in prognosis of human cholangiocarcinoma, Hum. Pathol. 41 (2010) 415–424.

[21] R.L. Siegel, K.D. Miller, A. Jemal, Cancer statistics, 2018, CA, A Cancer Journal for Clinicians 68 (2018) 7–30.

[22] S.S. Mohapatra, S.K. Batra, S. Bharadwaj, M. Bouvet, B. Cosman, A. Goel, W. Jogunoori, M.J. Kelley, L. Mishra, B. Mishra, S. Mohapatra, B. Patel, J.R. Pisegna, J.P. Raufman, S. Rao, H. Roy, M. Scheuner, S. Singh, G. Vidyarthi, J. White, Precision medicine for CRC patients in the veteran population: state-of-the-art, challenges and research directions, Dig. Dis. Sci. 63 (2018) 1123–1138.

[23] I. Zlobec, F. Molinari, M. Kovac, M.P. Bihl, H.J. Altermatt, J. Diebold, H. Frick, M. Germer, M. Horcic, M. Montani, G. Singer, H. Yurtsever, A. Zettl, L. Terracciano, L. Mazzucchelli, P. Saletti, M. Frattini, K. Heinimann, A. Lugli, Prognostic and predictive value of TOPK stratified by KRAS and BRAF gene alterations in sporadic, hereditary and metastatic colorectal cancer patients, Br. J. Canc. 102 (2010) 151–161.

[24] L.A. Mina, G.W. Sledge Jr., Rethinking the metastatic cascade as a therapeutic target, Nat. Rev. Clin. Oncol. 8 (2011) 325–332.

[25] M. Riihimaki, A. Hemminki, J. Sundquist, K. Hemminki, Patterns of metastasis in colon and rectal cancer, Sci. Rep. 6 (2016) 29765.

[26] J.D. Brown-Clay, D.N. Shenoy, O. Timofeeva, B.V. Kallakury, A.K. Nandi, P.P. Banerjee, PBK/TOPK Enhances Aggressive Phenotype in Prostate Cancer via Beta-catenin-TCF/LEF-mediated Matrix Metalloproteinases Production and Invasion.

[27] J.D. Brown-Clay, D.N. Shenoy, O. Timofeeva, B.V. Kallakury, A.K. Nandi, P.P. Banerjee, PBK/TOPK enhances aggressive phenotype in prostate cancer via beta-catenin-TCF/LEF-mediated matrix metalloproteinases production and invasion, Oncotarget 6 (2015) 15594–15609.

[28] H. Yoon, J.P. Dehart, J.M. Murphy, S.T. Lim, Understanding the roles of FAK in cancer: inhibitors, genetic models, and new insights, J. Histochem. Cytochem. : official journal of the Histochemistry Society 63 (2015) 114–128.

[29] Y. Li, Z. Yang, W. Li, S. Xu, T. Wang, T. Wang, M. Niu, S. Zhang, L. Jia, S. Li, TOPK

promotes lung cancer resistance to EGFR tyrosine kinase inhibitors by phosphorylating and activating c-Jun, Oncotarget 7 (2016) 6748–6764.
[30] J.H. Park, H. Inoue, T. Kato, M. Zewde, T. Miyamoto, Y. Matsuo, R. Salgia, Y. Nakamura, TOPK (T-LAK cell-originated protein kinase) inhibitor exhibits growth suppressive effect on small cell lung cancer, Cancer Sci. 108 (2017) 488–496.
[31] D.J. Kim, Y. Li, K. Reddy, M.H. Lee, M.O. Kim, Y.Y. Cho, S.Y. Lee, J.E. Kim, A.M. Bode, Z. Dong, Novel TOPK inhibitor HI-TOPK-032 effectively suppresses colon cancer growth, Cancer Res. 72 (2012) 3060–3068.
[32] G. Gao, T. Zhang, Q. Wang, K. Reddy, H. Chen, K. Yao, K. Wang, E. Roh, T. Zykova, W. Ma, J. Ryu, C. Curiel-Lewandrowski, D. Alberts, S.E. Dickinson, A.M. Bode, Y. Xing, Z. Dong, ADA-07 suppresses solar ultraviolet-induced skin carcinogenesis by directly inhibiting TOPK, Mol. Canc. Therapeut. 16 (2017) 1843–1854.
[33] N. Dayal, C. Opoku-Temeng, D.E. Hernandez, M.A. Sooreshjani, B.A. Carter-Cooper, R.G. Lapidus, H.O. Sintim, Dual FLT3/TOPK inhibitor with activity against FLT3-ITD secondary mutations potently inhibits acute myeloid leukemia cell lines, Future Med. Chem. 10 (2018) 823–835.
[34] J. Yang, D. Yuan, T. Xing, H. Su, S. Zhang, J. Wen, Q. Bai, D. Dang, Ginsenoside Rh2 inhibiting HCT116 colon cancer cell proliferation through blocking PDZ-binding kinase/T-LAK cell-originated protein kinase, J Ginseng Res 40 (2016) 400–408.
[35] N.J. Kang, K.W. Lee, B.H. Kim, A.M. Bode, H.J. Lee, Y.S. Heo, L. Boardman, P. Limburg, H.J. Lee, Z. Dong, Coffee phenolic phytochemicals suppress colon cancer metastasis by targeting MEK and TOPK, Carcinogenesis 32 (2011) 921–928.
[36] Y. Matsuo, J.H. Park, T. Miyamoto, S. Yamamoto, S. Hisada, H. Alachkar, Y. Nakamura, TOPK Inhibitor Induces Complete Tumor Regression in Xenograft Models of Human Cancer through Inhibition of Cytokinesis.
[37] T. Anastassiadis, S.W. Deacon, K. Devarajan, H. Ma, J.R. Peterson, Comprehensive assay of kinase catalytic activity reveals features of kinase inhibitor selectivity, Nat. Biotechnol. 29 (2011) 1039–1045.
[38] D. Martinez Molina, R. Jafari, M. Ignatushchenko, T. Seki, E.A. Larsson, C. Dan, L. Sreekumar, Y. Cao, P. Nordlund, Monitoring drug target engagement in cells and tissues using the cellular thermal shift assay, Science 341 (2013) 84–87.
[39] F. Zhu, T.A. Zykova, B.S. Kang, Z. Wang, M.C. Ebeling, Y. Abe, W.Y. Ma, A.M. Bode, Z. Dong, Bidirectional signals transduced by TOPK-ERK interaction increase tumorigenesis of HCT116 colorectal cancer cells, Gastroenterology 133 (2007) 219–231.
[40] R. Sears, G. Leone, J. DeGregori, J.R. Nevins, Ras enhances Myc protein stability, Mol. Cell 3 (1999) 169–179.
[41] M.R. Junttila, J. Westermarck, Mechanisms of MYC stabilization in human malignancies, Cell Cycle 7 (2008) 592–596.
[42] S. Matsumoto, Y. Abe, T. Fujibuchi, T. Takeuchi, K. Kito, N. Ueda, K. Shigemoto, K. Gyo, Characterization of a MAPKK-like protein kinase TOPK, Biochem. Biophys. Res. Commun. 325 (2004) 997–1004.
[43] N.N. Kreis, F. Louwen, J. Yuan, Less understood issues: p21(Cip1) in mitosis and its therapeutic potential, Oncogene 34 (2015) 1758–1767.
[44] J.H. Park, D.S. Yoon, H.J. Choi, D.H. Hahm, S.M. Oh, Phosphorylation of IkappaBalpha at serine 32 by T-lymphokine-activated killer cell-originated protein kinase is essential for chemoresistance against doxorubicin in cervical cancer cells, J. Biol. Chem. 288 (2013) 3585–3593.
[45] V. Deschoolmeester, M. Baay, P. Specenier, F. Lardon, J.B. Vermorken, A review of the most promising biomarkers in colorectal cancer: one step closer to targeted therapy, Oncol. 15 (2010) 699–731.